Observational Study

Medicine®

OPEN

Clinico-radiological features of brain metastases from thyroid cancer

Song Soo Kim, MD[a], Seok-Mo Kim, MD[b], Mina Park, MD[a], Sang Hyun Suh, MD[a], Sung Jun Ahn, MD[a,*]

Abstract

The brain is an unusual site for distant metastases of thyroid cancer. The radiological features of brain metastases (BMs) have rarely been reported. Hemorrhage is frequently noted in BMs from thyroid cancer. This study aimed to investigate the clinico-radiological features of BMs from thyroid cancer and to determine the risk factors to predict BM hemorrhage.

We retrospectively evaluated the MR images of 35 patients with BMs from thyroid cancer at our hospital from 2013 to 2020. The number, size, site, presence of extra-cranial metastasis, presence of perilesional edema, intra-tumoral hemorrhage, enhancement pattern, and presence of diffusion restriction on MRI were described. We further classified the thyroid cancers into hemorrhagic and nonhemorrhagic groups to investigate the factors associated with hemorrhage.

54.29% of patients with thyroid BMs (19/35) had neurologic symptoms. 94.29% of patients (33/35) had extra-cranial metastases. The most common histology of primary thyroid cancer was papillary thyroid cancer (71.43%, 25/35), followed by anaplastic thyroid cancer (22.86%, 8/35). Thyroid cancer BMs were located mostly in the supra-tentorium (51.43%, 18/35) or both the supra and infra-tentorium (45.71%, 16/35). 60% of patients (21/35) showed hemorrhage within the BMs. The strongest predictor for BM hemorrhage was tumor size (variable importance: 50).

Thyroid cancer BMs exhibit a bleeding tendency. Furthermore, larger BMs are more likely to have an intra-tumoral hemorrhage.

Abbreviations: BM = brain metastasis, PTC = papillary thyroid cancer.

Keywords: brain metastasis, intra-tumoral hemorrhage, radiological features, thyroid cancer

1. Introduction

Thyroid cancer is the most common endocrine malignancy, with a rapidly increasing incidence rate.[1,2] Common subtypes of thyroid cancer are papillary thyroid cancer (PTC), follicular thyroid cancer, medullary thyroid cancer, and anaplastic thyroid cancer.[3] PTC, the most common subtype, has a relatively favorable prognosis with a 10-year survival rate of more than 90%.[4,5] PTC tends to remain confined to the thyroid gland, and brain metastasis (BM) is rare, occurring in 0.3% to 1.4% of patients;[6,7] however, these patients exhibit poor survival rates ranging from 7 to 33 months.[8,9] Furthermore, anaplastic thyroid cancer demonstrates both a higher frequency of multifocal BMs and significantly shorter survival rates once BM is diagnosed than that associated with differentiated thyroid carcinomas.[10]

Cancers of the lung (20%–56% of patients), breast (5%–20%), and skin (7%–16%) have the highest incidences of BMs.[11,12] Recently, a machine-learning classifier was able to predict the BM tumor type with high accuracy using MR radiomic features.[13] The radiological features of BMs from lung and breast cancer, including specific subtypes, have been reported.[14–18] Conversely, the radiological features of thyroid cancer BMs have rarely been reported.

Additionally, we observed that thyroid cancer BMs are associated with a higher frequency of hemorrhage, a complication in 14% of patients with BMs. It can further cause intracerebral hemorrhage, leading to serious neurologic deterioration.[19] Moreover, the treatment plan must be changed in the case of BMs because stereotactic radiosurgery may be associated with hemorrhage.[20–22]

Thus, in this study, we investigated the clinico-radiological features of BMs from thyroid cancer and tried to determine any risk factors for predicting BM hemorrhage.

2. Materials and methods

2.1. Study participants

This retrospective study was approved by the institutional review board of our hospital, and the requirement for informed consent

Editor: Chinnadurai Mani.

This study was supported by a National Research Foundation of Korea (NRF) grant funded by the Korean government (MSIT) (No. 2020R1F1A1056512) and a faculty research grant from the Yonsei University College of Medicine (6-2019-0050).

The study was approved by the institutional research ethics committee of XXX hospital and informed consent was waived due to the retrospective nature of the study.

The authors have no conflicts of interests to disclose.

The datasets generated during and/or analyzed during the current study are available from the corresponding author on reasonable request.

[a] Department of Radiology, Gangnam Severance Hospital, Yonsei University, College of Medicine, Seoul, Korea, [b] Department of Surgery, Gangnam Severance Hospital, Yonsei University, College of Medicine, Seoul, Korea.

[*] Correspondence: Sung Jun Ahn, Department of Radiology, Gangnam Severance Hospital, Yonsei University College of Medicine, 211 Eonju-ro, Gangnam-gu, Seoul 06273, Republic of Korea (e-mail: aahng77@yuhs.ac).

How to cite this article: Kim SS, Kim SM, Park M, Suh SH, Ahn SJ. Clinico-radiological features of brain metastases from thyroid cancer. Medicine 2021;100:48(e28069).

Received: 2 June 2021 / Received in final form: 28 October 2021 / Accepted: 12 November 2021

http://dx.doi.org/10.1097/MD.0000000000028069

was waived. We retrospectively reviewed the data from 38 patients with BMs from thyroid cancer, who underwent gadolinium-enhanced brain MRI at our institution between January 2013 and December 2020. We excluded 3 patients with thyroid cancer because they had other malignant diseases. Finally, a total of 35 patients with thyroid cancer BMs were included in this study. The thyroid cancer was histopathologically diagnosed based on thyroidectomy.

2.2. MRI and image analysis

All MR images were obtained using a GE 3T Discovery MR750 (GE Healthcare, Milwaukee, WI, USA) or a Siemens 3T Vida (Siemens Healthineers, Erlangen, Germany). Our brain MRI protocol for the GE 3T scanner included axial T2-weighted images (TR/TE, 6380/108 ms; FOV, 250 mm; voxel size, $0.7 \times 0.7 \times 5.0$ mm), diffusion-weighted echo-planar sequences (TR/TE, 8000/65.6 ms; FOV, 240 mm; voxel size, $0.7 \times 0.7 \times 4.0$ mm; 3 directions; b-value 0 and 1000 s/mm^2), FLAIR (TR/TE/TI, 4000/80/2000 ms; FOV, 230 mm; voxel size, $0.7 \times 0.7 \times 5.0$ mm), and susceptibility-weighted angiography (TR/TE, 42.3/26 ms; FOV, 240 mm; voxel size, $0.9 \times 0.9 \times 2.0$ mm). Moreover, a T1-weighted 3D spoiled gradient-recalled echo sequence (TR/TE/TI, 8.3/3.3 ms, inversion time, 450 ms; FOV, 220 mm; voxel size, $0.43 \times 0.43 \times 1$ mm) was acquired after the administration of a compact bolus (0.2 mmol/kg) of gadobutrol at an injection rate of 5 mL/s. For the Siemens scanner, a corresponding sequence was used with similar MR parameters.

Two neuro-radiologists who were blinded to the clinical and histopathologic findings independently evaluated the MR images on the picture archiving and communication system workstation monitors with regard to the following characteristics: the number of metastatic lesions, mean size of the metastatic lesion, site in terms of supra/infra-tentorial, presence of extra-cranial metastasis, presence of peritumoral edema, presence of intra-tumoral hemorrhage, enhancement patterns, and presence of diffusion restriction. The size of the lesion was defined as its largest dimension in any plane on the MR image. Peri-tumoral edema was considered to be present if perilesional T2 high signal intensity was observed. Intra-tumoral hemorrhage was considered to be present if the lesion contained dark signals on susceptibility-weighted imaging or T2-weighted gradient-echo sequences. The enhancement pattern was considered homogenous if the lesion showed a uniform and confluent enhancement after the administration of gadolinium contrast and was considered heterogeneous if the enhancement was nonuniform. Diffusion restriction was considered to be present if the lesion showed high signal intensity on the diffusion-weighted imaging sequence and low signal intensity on the apparent diffusion coefficient sequence. All disagreements between the raters were resolved by consensus.

2.3. Statistical analysis

Our cohorts were divided into 2 groups: non-hemorrhagic BM and hemorrhagic BM. Age, sex, the existence of extracranial metastasis, symptom, time from diagnosis of primary cancer to BM development, histology, mean size of BM, the number of BMs, edema, hemorrhage, diffusion-weighted image, enhancement pattern, and site of BMs were compared between the 2 groups. Independent *t*-test was applied for continuous variables while Chi-Squared test or Fisher exact test was used for categorical variables. A decision tree model distinguishing the presence and absence of BM in the hippocampal avoidance region was built with the Classification and regression tree analysis. Classification and regression tree analysis selects the best predictor variable for splitting the data into 2 child nodes with maximal purity. The process is repeated recursively for each child node, until either the minimum size of the terminal node is reached, or no further split improves the purity of the terminal node.[2,3] A P value $<.05$ was considered significant. The inter-rater reliability was assessed using the intra-class correlation coefficient with a two-way random model of absolute agreement. All data analyses were performed using R version 3.5.3.

3. Results

3.1. Clinico-radiological features of thyroid cancer BMs

A total of 35 patients with thyroid cancer BMs were included in this study. The mean age at the diagnosis of BMs was 62.37 years, 54.29% of patients with BMs (19/35) were female and 54.29% of patients (19/35) showed neurologic symptoms. The most common symptom was weakness (n = 5), followed by dizziness (n = 3), gait disturbance (n = 2), headache (n = 2), cognitive dysfunction (n = 2), seizure (n = 1), sensory change (n = 1), visual disturbance (n = 1), dysarthria (n = 1), and diplopia (n = 1). The time interval from diagnosis of thyroid cancer to BM development was 101.43 ± 94.90 months. Extra-cranial metastases were found in 94.29% (33/35). The most common histology of thyroid cancer was papillary thyroid cancer (71.43%, 25/35), followed by anaplastic thyroid cancer (22.86%, 8/35), follicular thyroid cancer (2.86%, 1/35), and medullary thyroid cancer (2.86%, 1/35). The mean size of BMs was 1.23 ± 0.71 cm. Edema was observed in 73.53% of patients with BMs (25/35), heterogeneous enhancement in 62.86% (22/35), and negative findings on diffusion weighted image in 66.67% (20/35). The extent of BMs was limited (the number of BMs < 10) in 77.14% (27/35) patients and extensive (the number of BMs ≥ 10) in 22.86% (8/35) patients. Supratentorial involvement and infratentorial involvement were seen in 51.43% (18/35) and 2.86% (1/35) patients, respectively, and both supra and infra-tentorial involvement were seen in 45.71% (16/35).

3.2. Hemorrhagic versus nonhemorrhagic BMs from thyroid cancer

Clinico-radiological features were compared between the 2 groups (Table 1). The mean size of hemorrhagic BMs was larger than that of non-hemorrhagic BMs (1.39 ± 0.82 cm vs 1.00 ± 0.44, $P = .043$). The mean age of patients with hemorrhagic BMs was higher than that of patients with nonhemorrhagic BMs (64.90 ± 8.99 years vs 58.57 ± 11.11 years); however, it was not statistically significant ($P = .072$). Other clinico-radiological features were not significantly different between the 2 groups. Hemorrhage with the BMs was seen in 60% of patients (21/35) (Fig. 1). The mean size of BM was the first partitioning predictor in the decision tree model. All patients with BMs larger than 1.8 cm (100%, 8/8) demonstrated hemorrhage while 48% of patients with BMs less than 1.8 cm (13/27) showed hemorrhage (Fig. 2). Regarding the site of BM, 67% of patients with BMs less than 1.8 cm, located in the infra-tentorium or both supra and infra-tentorium (10/15) showed hemorrhage while 25% of patients with BMs less than 1.8 cm, located in the supra-tentorium (3/12)

Table 1

Demographics, histological and MRI findings of hemorrhagic brain metastases (BMs) and nonhemorrhagic BMs in patients with thyroid cancer.

Characteristics	Total (N = 35)	Non-hemorrhagic BM (N = 14)	Hemorrhagic BM (N = 21)	*P* value
Clinical variables				
Age (yr)	62.37 ± 10.23	58.57 ± 11.11	64.90 ± 8.99	.072
Sex				.945
Female	19 (54.29%)	7 (50.00%)	12 (57.14%)	
Male	16 (45.71%)	7 (50.00%)	9 (42.86%)	
Extracranial metastasis				.656
No	2 (5.71%)	0 (0.0%)	2 (9.52%)	
Yes	33 (94.29%)	14 (100.00%)	19 (90.48%)	
Symptom				.446
No	16 (45.71%)	8 (57.14%)	8 (38.10%)	
Yes	19 (54.29%)	6 (42.86%)	13 (61.90%)	
Time from diagnosis to BM (months)	101.43 ± 94.90	91.50 ± 108.49	108.05 ± 86.86	.621
Histology				.21
Papillary	25 (71.43%)	8 (57.14%)	17 (80.95%)	
Follicular	1 (2.86%)	0 (0.0%)	1 (4.76%)	
Medullary	1 (2.86%)	1 (7.14%)	0 (0.0%)	
Anaplastic	8 (22.86%)	5 (35.71%)	3 (14.29%)	
MRI findings				
Mean size of BM (cm)	1.23 ± 0.71	1.00 ± 0.44	1.39 ± 0.82	.043
Number of lesions				
1–9	27 (77.14%)	11 (78.57%)	16 (76.19%)	1
>10	8 (22.86%)	3 (21.43%)	5 (23.81%)	
Edema				.531
Absence	9 (26.47%)	5 (35.71%)	4 (20.00%)	
Presence	25 (73.53%)	9 (64.29%)	16 (80.00%)	
DWI				
Negative	20 (66.67%)	8 (72.73%)	12 (63.16%)	.893
Positive	10 (33.33%)	3 (27.27%)	7 (36.84%)	
Enhancement				
Homogenous	13 (37.14%)	8 (57.14%)	5 (23.81%)	.101
Heterogeneous	22 (62.86%)	6 (42.86%)	16 (76.19%)	
Site				.382
Supratentorial	18 (51.43%)	9 (64.29%)	9 (42.86%)	
Infratenotorial	1 (2.86%)	0 (0.0%)	1 (4.76%)	
Both	16 (45.71%)	5 (35.71%)	11 (52.38%)	

*Indicates $P < 0.05$.

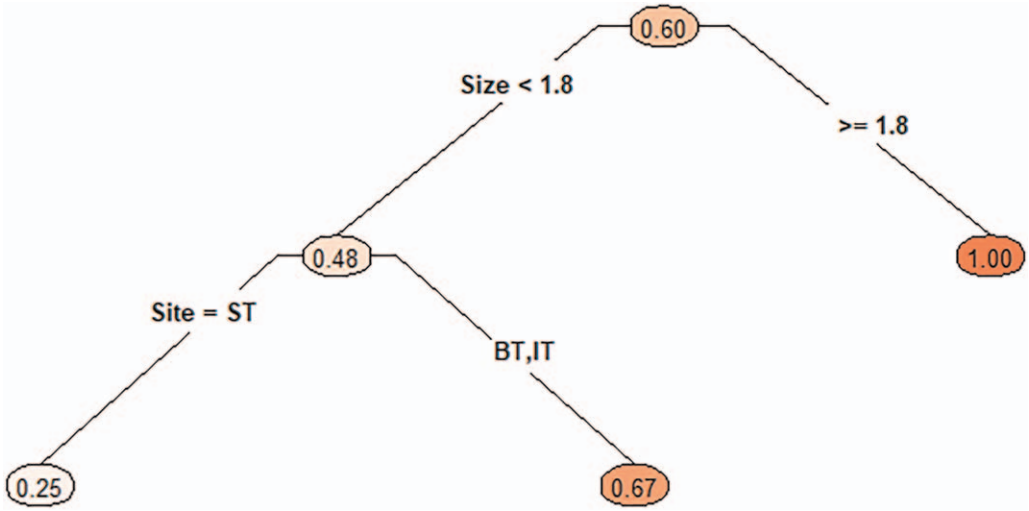

Figure 1. Classification and regression tree analysis (CART) results. The number inside the ellipse indicates the percentage of patients with hemorrhagic BMs among patients with thyroid cancer BMs.

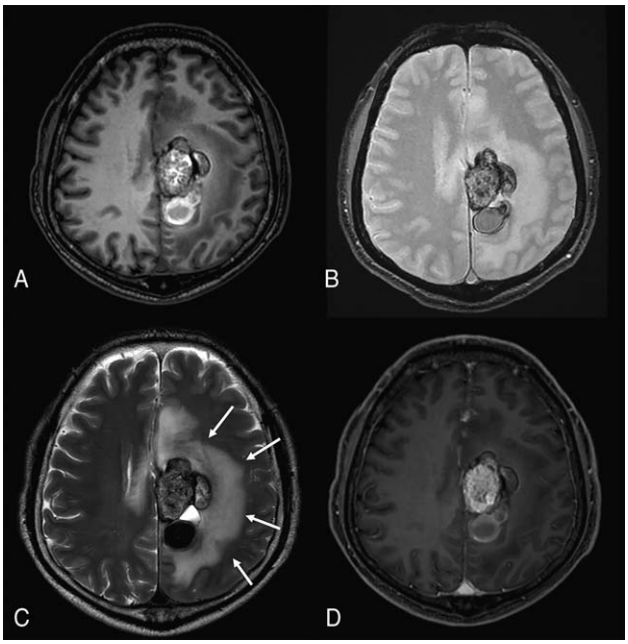

Figure 2. A 65-year-old man with pathologically confirmed papillary thyroid cancer. A 5.0-cm brain metastasis was detected 8 years after the diagnosis of the primary thyroid tumor. Intratumoral hemorrhage shows high signal intensity on T1-weighted imaging (T1WI) (A) and low signal intensity on T2* gradient echo sequences (B). Large peritumoral edema is seen on T2-weighted imaging (arrow) and heterogenous enhancement is observed on gadolinium-enhanced T1WI (D).

showed hemorrhage. The mean size of BMs showed the highest variable importance score followed by site, age, number of BMs, time from diagnosis to BM, and necrosis or cyst (Table 2).

4. Discussion

Our study indicates that 54.29% of patients with thyroid BMs exhibited neurologic symptoms. Most of them had extra-cranial metastases. The most common histology of primary thyroid cancer was papillary thyroid cancer (71.43%), followed by anaplastic thyroid cancer (22.86%). Thyroid cancer BMs were located mostly in the supra-tentorium or both supra and infra-tentorium, while BMs isolated within infra-tentorium were rare. Hemorrhage within the BMs was seen in 60% of the patients. The strongest predictor for BM hemorrhage was tumor size.

The clinico-radiological features of thyroid cancer BMs have been rarely reported. A study reported that 97% (46/47) patients showed neurologic symptoms.[10] However, a more recent study reported 58.3% of patients (14/24) had neurologic symptoms which was in line with our result.[6] The lower prevalence of patients with thyroid cancer BMs showing neurologic symptoms in recent studies may be explained by the more meticulous screening for BM regardless of the symptoms.

Table 2

Variable importance for the hemorrhagic BMs by classification and regression tree analysis.

Variable	Variable importance (%)
Mean size of BM	50
Site	27
Age	7
Number of BMs	7
Time from diagnosis to BM	5
Necrosis or cyst	5

In our study, thyroid cancer BMs showed a rather long interval (101 months) from the diagnosis of the primary tumor to the identification of the BM. Previous studies have reported a similar range of time intervals (34.8~127.2 months).[6,8,10] Additionally, our study demonstrated that extra-cranial metastasis was detected in 94.29% of patients with thyroid cancer BMs. This result agrees with previous studies reporting that 23 out of 24 (95.8%) and 24 out of 26 (96%) thyroid cancer presented with extra-cranial metastases at the time of BM diagnosis.[6,8] These findings support the idea that thyroid cancer BMs may occur at a relatively later stage in the disease course.

The biased spatial distribution of thyroid cancer BMs was noticeable. In our result, thyroid cancer BMs were not isolated within the cerebellum. The majority of BMs were located in the supra-tentorium or spread to the whole brain. The preferential involvement in certain regions has been reported in other primary cancers such as lung cancer and breast cancer.[24,25] Although the mechanism for the preferential involvement of specific brain regions remains unknown, we speculate that the "seed and soil theory" may partially explain it. The affinity of the tumor to the microenvironment plays a role in the extravasation and colonization of tumor cells at specific sites.[26]

The prevalence of hemorrhage in thyroid cancer was relatively high (60%), considering those of other tumors. Hemorrhage occurs in 3% to 14% of all cerebral metastases, which typically originate from renal cell carcinoma, melanoma, choriocarcinoma, bronchogenic carcinoma, and hepatocellular carcinoma.[27–29] This suggests that thyroid cancer should be considered in the differential diagnosis of hemorrhagic intracranial metastases. According to our study, the mean size of the BM was the strongest predictor for hemorrhage of thyroid cancer BMs. It is well-established that tumor necrosis increases with increasing tumor volume.[30,31] Vascular endothelial proliferation with thin-walled, poorly formed vessels in intra-tumoral necrosis may be associated with intra-tumoral hemorrhage.[28] The bleeding tendency of BMs can also be affected by the histologic subtype of thyroid cancer. In our study, PTC was the most common histologic subtype of the hemorrhagic thyroid cancer BMs. This is in line with previous case series that have reported hemorrhagic BMs from PTC.[27,29,32,33] PTC is further divided into numerous subtypes based on genetic alterations.[34] The tall cell and columnar cell variants of PTC are biologically more aggressive.[35] However, we did not study the effect of the molecular subtype of PTC on the risk of hemorrhage because this information was not available to us.

The limitation of our study is its small sample size; our cohort was too small to draw a robust conclusion. However, considering the rarity of BMs from thyroid cancer, our study has a relatively larger number of cases than those reported in previous studies. Thus, our results may serve as a cornerstone for future studies with larger samples that can validate and extend the scope of our results.

5. Conclusion

Our study demonstrated that most patients with thyroid cancer BMs tend to have extra-cranial metastases and half of them experience neurologic symptoms. Thyroid cancer BMs exhibit a

bleeding tendency and preferential involvement of the supratentorium or spread to the entire brain. The common histological types to metastasize to the brain are papillary thyroid cancer and anaplastic thyroid cancer.

Author contributions

Conceptualization: Sung Jun Ahn.
Data curation: Seok-Mo Kim.
Investigation: Song Soo Kim, Mina Park, Sang Hyun Suh, Sung Jun Ahn.
Methodology: Mina Park, Sung Jun Ahn.
Supervision: Seok-Mo Kim, Sang Hyun Suh.
Writing – original draft: Song Soo Kim.
Writing – review & editing: Sung Jun Ahn.

References

[1] Fahiminiya S, de Kock L, Foulkes WD. Biologic and clinical perspectives on thyroid cancer. N Engl J Med 2016;375:2306–7.
[2] Lim H, Devesa SS, Sosa JA, Check D, Kitahara CM. Trends in thyroid cancer incidence and mortality in the United States, 1974-2013. JAMA 2017;317:1338–48.
[3] Fagin JA, Wells SA. Biologic and clinical perspectives on thyroid cancer. N Engl J Med 2016;375:1054–67.
[4] Sebastian SO, Gonzalez JM, Paricio PP, et al. Papillary thyroid carcinoma: prognostic index for survival including the histological variety. Arch Surg 2000;135:272–7.
[5] Schlumberger MJ. Papillary and follicular thyroid carcinoma. N Engl J Med 1998;338:297–306.
[6] Gomes-Lima CJ, Wu D, Rao SN, et al. Brain metastases from differentiated thyroid carcinoma: prevalence, current therapies, and outcomes. J Endocr Soc 2019;3:359–71.
[7] Henriques de Figueiredo B, Godbert Y, Soubeyran I, et al. Brain metastases from thyroid carcinoma: a retrospective study of 21 patients. Thyroid 2014;24:270–6.
[8] Choi J, Kim JW, Keum YS, Lee IJ. The largest known survival analysis of patients with brain metastasis from thyroid cancer based on prognostic groups. PLoS One 2016;11:e0154739.
[9] Samuel AM, Shah DH. Brain metastases in well-differentiated carcinoma of the thyroid. Tumori 1997;83:608–10.
[10] Chiu AC, Delpassand ES, Sherman SI. Prognosis and treatment of brain metastases in thyroid carcinoma. J Clin Endocrinol Metab 1997;82:3637–42.
[11] Nayak L, Lee EQ, Wen PY. Epidemiology of brain metastases. Curr Oncol Rep 2012;14:48–54.
[12] Sperduto PW, Chao ST, Sneed PK, et al. Diagnosis-specific prognostic factors, indexes, and treatment outcomes for patients with newly diagnosed brain metastases: a multi-institutional analysis of 4259 patients. Int J Radiat Oncol Biol Phys 2010;77:655–61.
[13] Kniep HC, Madesta F, Schneider T, et al. Radiomics of brain MRI: utility in prediction of metastatic tumor type. Radiology 2019;290: 479–87.
[14] Jena A, Taneja S, Talwar V, Sharma JB. Magnetic resonance (MR) patterns of brain metastasis in lung cancer patients: correlation of imaging findings with symptom. J Thorac Oncol 2008;3:140–4.
[15] Chu L, Ni J, Yang X, et al. Radiographic features of metastatic brain tumors from ALK-rearranged non-small cell lung cancer: implications for optimal treatment modalities. J Cancer 2019;10:6660–5.
[16] Jung WS, Park CH, Hong CK, Suh SH, Ahn SJ. Diffusion-weighted imaging of brain metastasis from lung cancer: correlation of MRI parameters with the histologic type and gene mutation status. AJNR Am J Neuroradiol 2018;39:273–9.
[17] Ahn SJ, Park M, Bang S, et al. Apparent diffusion coefficient histogram in breast cancer brain metastases may predict their biological subtype and progression. Sci Rep 2018;8:9947.
[18] Ahn SJ, Kwon H, Yang JJ, et al. Contrast-enhanced T1-weighted image radiomics of brain metastases may predict EGFR mutation status in primary lung cancer. Sci Rep 2020;10:8905.
[19] Maiuri F, D'Andrea F, Gallicchio B, Carandente M. Intracranial hemorrhages in metastatic brain tumors. J Neurosurg Sci 1985;29:37–41.
[20] Lavine SD, Petrovich Z, Cohen-Gadol AA, et al. Gamma knife radiosurgery for metastatic melanoma: an analysis of survival, outcome, and complications. Neurosurgery 1999;44:59–64. discussion 64-56.
[21] Redmond AJ, Diluna ML, Hebert R, et al. Gamma Knife surgery for the treatment of melanoma metastases: the effect of intratumoral hemorrhage on survival. J Neurosurg 2008;109 Suppl:99–105.
[22] Seung SK, Sneed PK, McDermott MW, et al. Gamma knife radiosurgery for malignant melanoma brain metastases. Cancer J Sci Am 1998;4:103–9.
[23] Lewis RJ. An introduction to classification and regression tree (CART) analysis. Annual meeting of the society for academic emergency medicine in San Francisco, California 2000.
[24] Kyeong S, Cha YJ, Ahn SG, Suh SH, Son EJ, Ahn SJ. Subtypes of breast cancer show different spatial distributions of brain metastases. PLoS One 2017;12:e0188542.
[25] Kwon H, Kim JW, Park M, et al. Brain metastases from lung adenocarcinoma may preferentially involve the distal middle cerebral artery territory and cerebellum. Front Oncol 2020;10:1664.
[26] Croucher PI, McDonald MM, Martin TJ. Bone metastasis: the importance of the neighbourhood. Nat Rev Cancer 2016;16:373.
[27] Chonan M, Mino M, Yoshida M, Sakamoto K. Brain metastasis from papillary thyroid carcinoma with acute intracerebral hemorrhage: a surgical case report. No Shinkei Geka 2012;40:453–7.
[28] Lieu AS, Hwang SL, Howng SL, Chai CY. Brain tumors with hemorrhage. J Formos Med Assoc 1999;98:365–7.
[29] Tanaka T, Kato N, Aoki K, et al. Cerebellar hemorrhage secondary to cerebellopontine angle metastasis from thyroid papillary carcinoma. Neurol Med Chir (Tokyo) 2013;53:233–6.
[30] Baker GM, Goddard HL, Clarke MB, Whimster WF. Proportion of necrosis in transplanted murine adenocarcinomas and its relationship to tumor growth. Growth Dev Aging 1990;54:85–93.
[31] Milross CG, Tucker SL, Mason KA, Hunter NR, Peters LJ, Milas L. The effect of tumor size on necrosis and polarographically measured pO2. Acta Oncol 1997;36:183–9.
[32] Lin CK, Lieu AS, Howng SL. Hemorrhagic cerebellar metastasis from papillary thyroid carcinoma. Kaohsiung J Med Sci 1999;15:234–8.
[33] Lecumberri B, Alvarez-Escola C, Martin-Vaquero P, et al. Solitary hemorrhagic cerebellar metastasis from occult papillary thyroid microcarcinoma. Thyroid 2010;20:563–7.
[34] Lloyd RV, Buehler D, Khanafshar E. Papillary thyroid carcinoma variants. Head Neck Pathol 2011;5:51–6.
[35] Adeniran AJ, Zhu Z, Gandhi M, et al. Correlation between genetic alterations and microscopic features, clinical manifestations, and prognostic characteristics of thyroid papillary carcinomas. Am J Surg Pathol 2006;30:216–22.